Joint Special Interest Group meeting between euspen and ASPE
Advancing Precision in Additive Manufacturing
Inspire AG, St. Gallen, Switzerland 2021
www.euspen.eu

# Surface irregularities of metal SLM part with different surface inclinations and their impact on surface texture characterization

S. Ramadurga Narasimharaju[1], W. Liu[1], W. Zeng[1], T. L. See[2], P. J. Scott[1], X. Jiang[1], S. Lou[1]

[1]*EPSRC Future Metrology Hub, University of Huddersfield, Queensgate, Huddersfield, UK*

[2]*Laser Processing Group, Manufacturing Technology Centre, Ansty Park, Coventry, UK*

*shubhavardhan.narasimharaju@hud.ac.uk*

**Abstract**

Additive manufacturing (AM) offers numerous advantages like unlimited freedom to design the most complicated parts without expensive support tools and moulds at reduced lead-times. However, AM is not completely established to meet compliance of industrial standards due to intrinsic fabrication process induced rougher surface quality and poor dimensional tolerance especially the inclined and curved AM components. It is paramount to address the evolution of surface irregularities such as the staircase effect, the spatters, the adhered un-melted or partially-melted particles that impart poor surface quality on the inclined and curved metal AM surfaces. Hence, this research is focused on investigating the emergence of surface irregularities and their impact on the resultant surface texture with respect to various surface inclination angles. Focus variation measurement (FVM) method is employed to acquire the surface topography of bespoke metal truncheon artefact produced by SLM with various surface inclinations from 0° to 180°. The areal surface texture characterization and the particle-based feature analysis reveal that there exists a strong intertwining relationship between the resulted surface topographies and the surface inclination angles.

**Keywords**

Selective laser melting (SLM), surface irregularities, varying surface inclinations, areal surface texture characterization.

## 1. Introduction

AM is gaining attention among researchers and manufacturers from aerospace, biomedical, automotive industrial fraternity, because light weight cellular and lattice type structures, various medical and dental implants, bionics are manufactured and used in functional applications [1]. In addition to the fabrication of complex light weight parts, a paradigm shift from mass production to mass customization are the new prospective of AM applications [1-3].

Although AM offers countless advantages, poor repeatability, dimensional accuracy and surface quality are the main factors that are limiting the rapid advancement of AM process [4]. It has been noted that surface quality (surface texture) is critical on the part functionality of conventional process, which account for the 10% of part failure rate [5], and it is estimated to be even more in case of AM processes [6]. AM surface quality is influenced by several factors like power of heat source, scan speed, hatch spacing, layer thickness, heat source incidence, part orientation, power size distribution etc. Amongst all layer thickness is a critical parameter responsible to establish the staircase effect particularly on curved and inclined metal AM parts [7,8]. Due to the complex thermophysical layer-by-layer approach of AM processes often induce rougher surface. It turns to be extremely hard to control the surface quality of curved or inclined AM components, which is generally dictated by inevitable surface irregularities such as ripple effect, staircase effect, spatters, un-melted, partially-melted powder particles [9-13]. It is utmost importance to address this prevailing condition pertaining to the surface quality of AM components. Hence, this research is focused to examine the intertwining relationship between the various surface irregularities emerge on the up-skin and down-skin surfaces of the truncheon artefact with different inclination angles.

## 2. Research methodology

### *2.1. SLM artefact design and fabrication*

Renishaw AM400 SLM machine was used to build truncheon artefact using 316L stainless steel alloy powder. The following SLM parameters were used, laser power 110W, scan speed 5000 mm/s, hatch spacing 110 µm, and layer thickness 50 µm. Artefact design contains 31 square sections (3° increments) with different inclination angles from 0° to 180° (Fig. 1a & 1b). 0°-90° surfaces are defined as the up-skin surfaces, whereas 90°-180° are denoted by the down-skin surfaces.

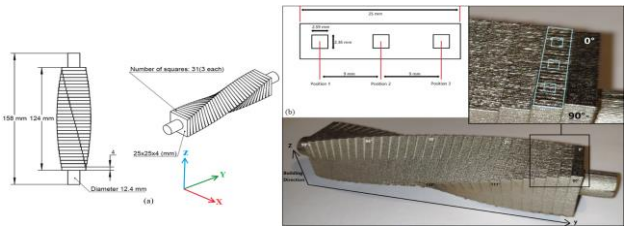


**Figure 1.** Schematic illustration of (a)Truncheon artefact drawing with dimensions, (b) SLM built artefact with measurement details

### *2.2. Measurement strategy*

Alicona G4 infinite FVM system was employed to measure areal topography of SLM artefact. However, down-skin surfaces measurement was limited to 132 °, beyond this all the surface inclinations were severely damaged by the support structures. FVM measurement configurations are: magnification lens 20X, ring light illumination, lateral resolution 1 µm, vertical resolution 0.7 µm, sampling distance 0.878 µm (in both X and Y directions), and measurement size 2.59 x 2.36 mm (stitched).

### *2.3. Data processing and surface texture characterization*

The captured data was analysed using Digital surf MountainsMap software. Fig. 2 shows the procedure of FVM data extraction and processing. The imported data is first processed by filling non-measurement points (NMP) followed by least square levelling. Resulted data is then filtered using the S-filter (nesting index 5 µm) to remove short spatial wavelength components like noise. Similarly, to separate particle features from underlying staircase surface, robust gaussian filter with nesting index 80 µm was applied due to its robustness against outliers [14]. The analysed data is useful to interpret staircase effect and particle features.

The spectrum of ISO 25178-2 areal surface texture parameters adopted to interpret surface topographical features are height parameters, spatial parameters, functional parameters, hybrid parameters, feature parameters, and particles analysis [15] (see Table 1).

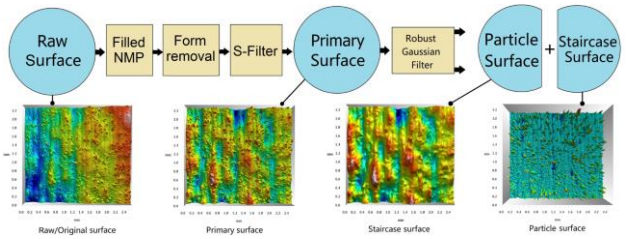


**Figure 2.** Extraction of primary, staircase and particle surfaces using suitable filters

**Table 1** List of areal surface texture parameters explored in this research

| Categories | Surface texture parameters |
|---|---|
| Height Parameters | Sa (µm) -Arithmetical mean height |
| | Sq (µm) -Root mean square height |
| | Ssk -Skewness |
| | Sku- Kurtosis |
| Hybrid Parameters | Sdq -Root mean square gradient |
| | Sdr (%) -Developed interfacial area ratio |
| Functional parameters | Smr1 (%) -Material ratio related to the peak zone |
| | Vmp ($mm^3/mm^2$) -Peak material volume |
| Spatial Parameters | Sal (µm) -Autocorrelation length |
| | Str -Texture aspect ratio |
| Feature parameters | Spd ($1/mm^2$) Density of peaks |
| Particles analysis | Particles number/density/coverage |

### 2.4 Surface roughness prediction model

A mathematical model based on trigonometric modelling of the staircase effect was adopted [16], to predict the staircase features of SLM truncheon artefact. The roughness based on the trigonometric modelling functions is given by Eq. (1), where 'Lt' is layer thickness, and 'α' is inclination angle (with reference to the building surface and edge of the stair-step). Computer-aided design (CAD) software was used to generate the ideal 3D inclined surfaces based on the trigonometric model (see Fig. 3). Selected layer thickness (50 µm) is the same value used while fabricating SLM test artefact. Since the ideal faces 0°–90° and 90°–180° comprise symmetrical features, only 0°–90° range is considered with increments of 3°. Areal surface texture parameters (Sa, Sq, Ssk, Sku, and Sal) values of ideal surfaces are calculated and compared with the actual measurements.

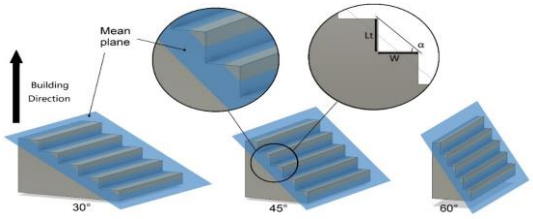


**Figure 3.** Three-dimensional (3D) representation of the prediction CAD model to illustrate the staircase effect.

$$\mathrm{Ra} = \frac{1}{L}\int_0^L |y(x)|d \;=\; \frac{1}{4}L_t\cos(\alpha) \qquad (1)$$

## 3. Results and discussions

### 3.1 Height parameters

Sa and Sq plots for primary and staircase surfaces demonstrate identical trends for all inclination angles (see Fig. 4 & 5). A higher indeterminacy can be observed at 0°, which could be related to the ripple effect caused by the rapid movement of laser. Rapid increase in surface roughness between 3°-6° is attributed to the staircase effect, which steadily decreased till 45°. Beyond this inclination angle, staircase effect started to disappear and was completely replaced by adhered particles at 90°. An increasing roughness for all down-skin surfaces is clearly evident (~140%), credited to the increased number of adhered particles due to intermittent heat transfer.

A quick change in predicted Sa and Sq from 0°-3° is credited to the transition from a flat surface to a strong staircase induced surface. A constant declining trend thereafter between 3°-90° is attributed to the decreasing strength of the staircase effect. This is followed by an increasing trend after 90° (down-skin surfaces) due to the re-appearance of the staircase effect in opposite direction. Overall, Sa and Sq trends of the measurements for all cases tend to closely follow the theoretical mathematical model.

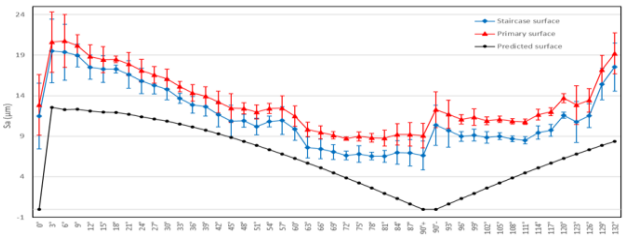


**Figure 4**. Sa values for predicted, primary and staircase surfaces

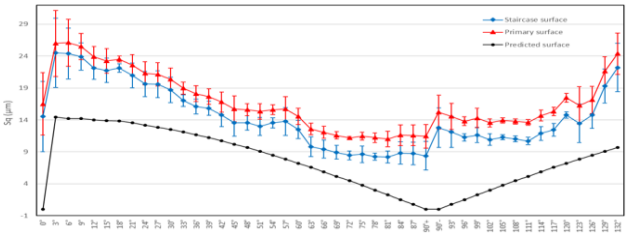


**Figure 5**. Sq values for predicted, primary and staircase surfaces

The majority of Ssk remained to be positive for all up-skin surfaces, signifying mostly peaks dominates the surface, while the Ssk tend to be unstable for down-skin surfaces, plus negative skew reported at 114°. This is ascribed to the deep valleys and redundant peak features (see Fig. 6). A closer look in to prediction model reveal, the Ssk values are nearly zero, because the number of peaks and valleys is considered to be the same.

Sku values for all surface inclinations tend to be marginally above the nominal value 3, indicating surface height distribution is basically a spiky natured normal distribution (see Fig. 7). Predicted surface displays a Sku value lesser than 3 for all the cases, plus there are no peaks and valleys at 0°, 90°, and 180°; hence, Sku is considered to be infinite in these cases.

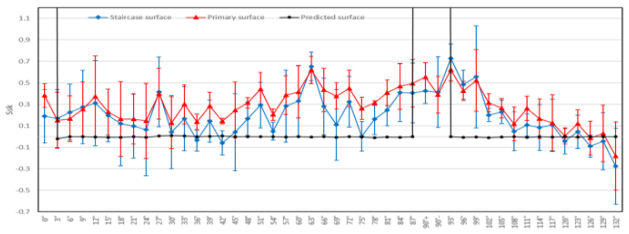


**Figure 6**. Ssk of predicted, primary and staircase surfaces

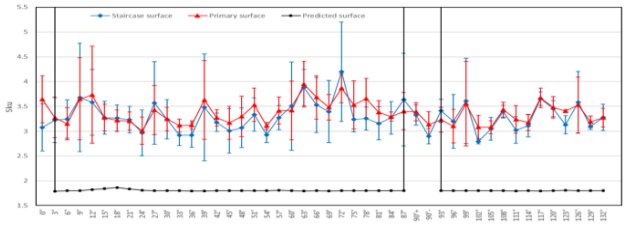


**Figure 7**. Sku values for predicted, primary and staircase surfaces

### 3.2 Spatial parameters

Sal is defined by the shortest autocorrelation length of the new location with respect to the original location. Sal displays an oscillating pattern overall, see Fig. 8. A closer view demonstrates a decreasing trend for the up-skin surfaces, whilst an increasing trend for the down-skin surfaces. This characteristic is consistent with the fact that the width of staircase reduces towards 90°. If the particle features remain on the staircase surface then it can introduce significant turbulence in Sal trend.

Sal for the predicted surface displays a very interesting trend consisting of a sharp steep peak at 3°, and a steady decline to become flat at 90°. Based on the prediction model, Sal decreases with the increase of the inclination angle, which completely aligns with the reduction of the step width illustrated in Fig. 9. The predicted surface at 0° presents a completely flat surface (melt tracks are not taken into consideration); thus, Sal is zero. This is same in the case of 90° (no staircase at all). Sal of the predicted down-skin surface maps the changing trend of the up-skin surface by reflection in terms of 90°.

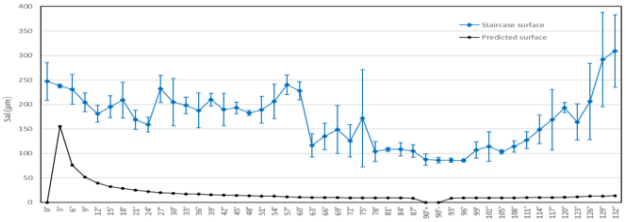


**Figure 8**. Sal values of predicted surface staircase surface

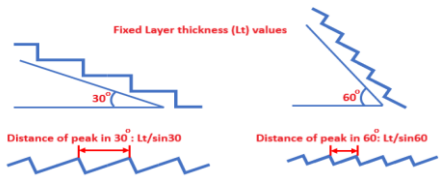


**Figure 9**. Schematic illustration of change in staircase width

Str (texture aspect ratio) is a measure of uniformity of a surface texture. Str for the particle surface remained almost stable (except between 0° & 27°) with the values approaching to 1; indicating the isotropic nature of particles (see Fig. 10). Str for both the primary and staircase surfaces displayed similar fluctuating trends (like Sal) with the value close to 0 signifying the anisotropic characteristics of these two surfaces. The staircase effect is the main factor that affects Str.

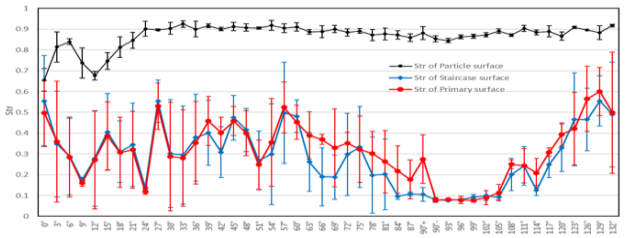


**Figure 10**. Str of primary, staircase surface and particles surface.

### 3.3 Hybrid parameters

Sdr is mainly used in surface coating, lubrication and heat exchanger applications, where functional performance is linked to surface area. Sdr results for the primary and staircase surfaces displayed identical trends and the specific values are very close, signifying the staircase effect is less significant (see Fig. 11). Key for Sdr results is the adhered particle features.

Sdq is usually employed to distinguish the surfaces with similar roughness. Sdq results between 0°-90° showed a minor increasing oscillation pattern, whereas the down-skin surfaces exhibit a V-shaped trend. Overall, the changing trend of the up-skin surface Sdq is relatively uniform, whilst the down-skin surface is more turbulent (see Fig. 12).

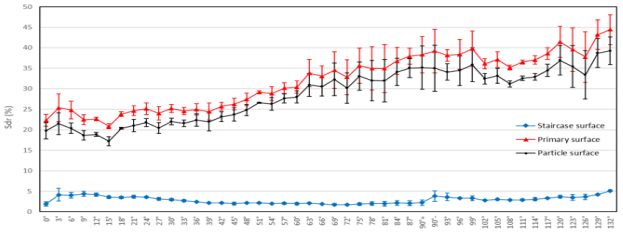


**Figure 11**. Sdr of primary, staircase surface and particles surface.

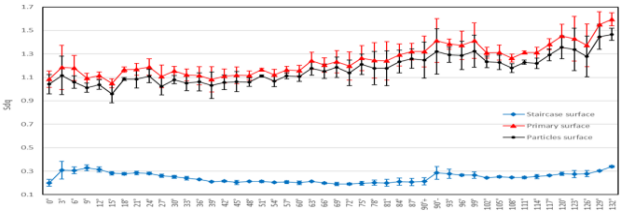


**Figure 12**. Sdq of primary, staircase surface and particles surface.

### 3.4 Functional parameters

Functional parameters are developed to characterize the functional characteristics like wear and tribological properties. The peak material volume parameter (Vmp) used to investigate the volume density of particle features. Steady increase in Vmp for all up-skin surfaces is attributed to the increasing adherence of un-melted, partially melted particles onto the edges of the stair steps (see Fig. 13). The down-skin surfaces did not display any interesting fact except irregular changing pattern.

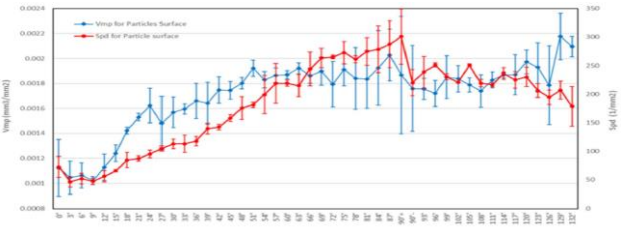


**Figure 13**. Vmp and Spd of particles surface.

### 3.5 Feature parameters

Spd, signifying the density of peaks, is based on the watershed segmentation of surface topography with 5% Wolf pruning . Spd and Vmp of particle surface with respect to varying inclination angles is shown in Fig. 13. Spd decreases between 0°-3° which is related to the spatters. Down-skin surface presents a steady decrease of Spd, which forms a certain reflection symmetry to the up-skin surfaces but showing more variations due to the random nature of the down-skin surface topography. By comparing the trend of down-skin surface Spd and Vmp: Spd decreases as the down-skin inclination increases, whereas it is the polar opposite in the case of Vmp. This implies as the down-skin tilt angle increases, the number of large particles or large protrusions on the bottom surface increases.

### 3.6 Particle analysis

Complimentary to Spd, height threshold segmentation approach is applied to the particle surface (staircase effect has been excluded). The cut-off is set to Smr1 by presuming the peak zone stands for the particle features [17]. The number of particles, the particle coverage, and the particle density are calculated respectively to provide quantitative characterization of particles, which displayed similar trends (see Fig. 14 & 15). These three particle characterization parameters of the up-skin surfaces increased slowly, while those for down-skin surfaces demonstrated a flatter pattern.

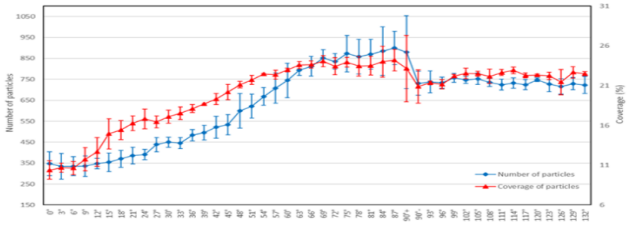


**Figure 14.** Number of particles, particle coverage of the particle surface

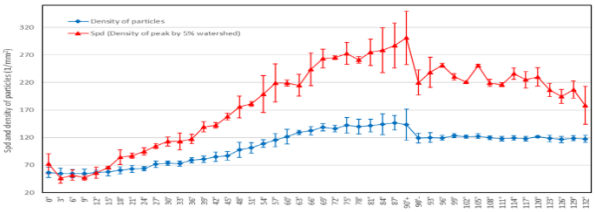


**Figure 15.** Particle density and Spd of the particle surface

Six examples of features-based particle identification and associated particle coverage ratio and numbers are illustrated in Fig. 16. On the up-skin surface, the number of stair steps increases as the inclination goes up, while the corresponding width of these steps gradually decreases. This causes a rising number of particles to adhere to the edges of the steps. The number of particles and the particle coverage rate on the down-skin surfaces remain relatively steady, which is attributed to the intermittent heat transfer and the gravity effects.

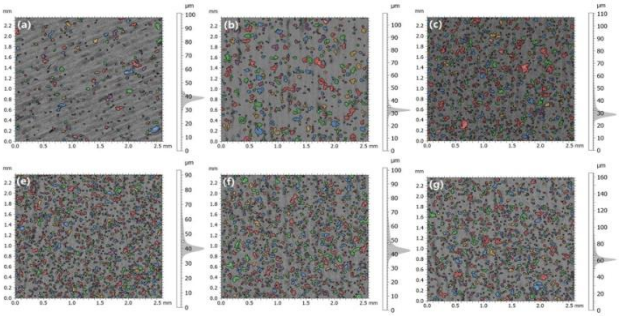


**Figure 16**. Particles identification for six inclined surfaces: (a) 0 deg, 314 particles, 10.20% coverage; (b) 30 deg, 394 particles;18.34% coverage; (c) 60 deg, 685 particles, 24.36% coverage; (d) 90 deg+, 848 particles, 27.28% coverage; (e) 114 deg, 717 particles,24.65% coverage; and (f) 132 deg, 707 particles, 24.33% coverage

### 4. Conclusions

The correlation between the various surface irregularities and different build inclination angles of a SLM built artefact was investigated. Appropriate surface texture parameters were used to characterize and quantify the various surface irregularities:

Sa and Sq values of inclined surfaces are mainly governed by the staircase effect, whilst the influence of adhered particles is less significant. Additionally, Sa and Sq of the down-skin surfaces were higher as compared to the up-skin surfaces due to the intermittent heat transfer. Sa and Sq trends for all cases tend to closely follow the prediction model. Ssk values tend to be mostly positive, signifying the surface is dominated by peak features and displayed similar pattern for up-skin and down-skin surfaces. Recorded Sku was marginally above the nominal value 3, indicating the surface height distribution was basically spiky-natured normal distribution.

Sal is predominantly influenced by the staircase effect; the staircase width decreases with the increase of inclination angle. However, Sal could also be affected by the residue traces of particles on the staircase surface.

Sdr and Sdq of the primary surface and the particle surface displayed strong increasing trend as the inclination angles increased, implying that particle features are responsible for the increase in surface area and general surface slope. The impact of the staircase effect is insignificant.

Vmp (threshold ratio set to Smr1), exhibited strong upward trend with increasing inclination angles, denoting surfaces with higher inclinations showed larger total volume of particles.

Spd for particles surface showed the upward trend for the up-skin surfaces, signifying growth of particle features, whereas down-surfaces displayed an opposite trend.

The particle analysis descriptors of particles surface revealed steady rising trend for the up-skin surfaces, and relatively stable trend for the down-skin surfaces. Overall, the descriptors exhibited consistent trends.


### Acknowledgements

S. Lou would like to acknowledge the support of EPSRC via New Investigator Award (EP/S000453/1) Catapult RiR (EP/R513520/1), and the support of the 3M Buckley Innovation Centre via 3M BIC Fellowship. The authors from the University of Huddersfield gratefully acknowledge EPSRC funding of the Future Advanced Metrology Hub (EP/P006930/1).


### References


[1] Mehrpouya, M., Dehghanghadikolaei, A., Fotovvati, B., Vosooghnia, A., Emamian, S.S. and Gisario, A., 2019. **9**(18), p.3865.

[2] Brooks, W.K., Tsopanos, S., Stamp, R., Sutcliffe, C.J., Cantwell, W.J., Fox, P. and Todd, J., 2005, June. University, Lancaster, UK (Vol. **10**).

[3] Li, X., Tan, Y.H., Willy, H.J., Wang, P., Lu, W., Cagirici, M., Ong, C.Y.A., Herng, T.S., Wei, J. and Ding, J., 2019. Materials & Design, **178**, p.107881

[4] Kannan, G.B. and Rajendran, D.K., 2017. (pp. 95-100). Springer, Singapore.

[5] R. Leach, "Optical Measurement of Surface Topography" 2011 Springer-Verlag Berlin Heidelberg. DOI 10.1007/978-3-642-12012-1

[6] Grimm, T., Wiora, G. and Witt, G., 2015. metrology and properties, **3**(1), p.014001.

[7] Triantaphyllou, A., Giusca, C.L., Macaulay, G.D., Roerig, F., Hoebel, M., Leach, R.K., Tomita, B. and Milne, K.A., 2015 Surface topography: metrology and properties, **3**(2), p.024002.

[8] Watson, D.A., 1999. (Doctoral dissertation, University of Texas at Austin).

[9] Tang, P., Wang, S., Duan, H., Long, M., Li, Y., Fan, S. and Chen, D., 2020. JOM, **72**(3), pp.1128-1137.

[10] Yasa, E., Deckers, J. and Kruth, J.P., 2011. Rapid Prototyping Journal.

[11] Song, B., Dong, S.J., Liao, H.L. and Coddet, C., 2012. Materials Research Innovations, **16**(5), pp.321-325.

[12] Yadroitsev, I., Krakhmalev, P., Yadroitsava, I., Johansson, S. and Smurov, I., 2013Journal of Materials Processing Technology, **213**(4), pp.606-613.

[13] Galicki, D., List, F., Babu, S.S., Plotkowski, A., Meyer, H.M., Seals, R. and Hayes, C., 2019. Metallurgical and Materials Transactions A, **50**(3), pp.1582-1605.

[14] Lou, S., Jiang, X., Sun, W., Zeng, W., Pagani, L., and Scott, P. J., 2019, Precis. Eng., **57**, pp. 1–15.

[15] Ramadurga Narasimharaju, S., Liu, W., Zeng, W., See, T. L., Scott, P., Jiang, X., & Lou, S. *Journal of Tribology*, 1-37

[16] Reeves, P. E., and Cobb, R. C., 1995, Proceedings of Fifth European Conference on Rapid Prototyping and Manufacturing.

[17] Lou, S., Zhu, Z., Zeng, W., Majewski, C., Scott, P. J., & Jiang, X. (2021). Surface Topography: Metrology and Properties, **9**(1), 015029.